Annals of Botany Page 1 of 13
doi:10.1093/aob/mcu232, available online at www.aob.oxfordjournals.org

ANNALS OF BOTANY
Founded 1887

Immunolabelling of intervessel pits for polysaccharides and lignin helps in understanding their hydraulic properties in *Populus tremula* × *alba*

Stéphane Herbette[1,2,*], Brigitte Bouchet[3], Nicole Brunel[1,2], Estelle Bonnin[3], Hervé Cochard[2,1] and Fabienne Guillon[3]

[1]Clermont Université, Université Blaise Pascal, UMR547 PIAF, BP 10448, F-63000 Clermont-Ferrand, France, [2]INRA, UMR547 PIAF, F-63100 Clermont-Ferrand, France and [3]INRA, UR1268 Biopolymers Interactions Assemblies, BP 71627, F-44316 Nantes, France

** For correspondence. E-mail stephane.herbette@univ-bpclermont.fr*

Received: 8 September 2014 Returned for revision: 22 September 2014 Accepted: 9 October 2014

• **Background and Aims** The efficiency and safety functions of xylem hydraulics are strongly dependent on the pits that connect the xylem vessels. However, little is known about their biochemical composition and thus about their hydraulic properties. In this study, the distribution of the epitopes of different wall components (cellulose, hemicelluloses, pectins and lignins) was analysed in intervessel pits of hybrid poplar (*Populus tremula* × *alba*).
• **Methods** Immunogold labelling with transmission electron microscopy was carried out with a set of antibodies raised against different epitopes for each wall polysaccharide type and for lignins. Analyses were performed on both immature and mature vessels. The effect of sap ionic strength on xylem conductance was also tested.
• **Key Results** In mature vessels, the pit membrane (PM) was composed of crystalline cellulose and lignins. None of the hemicellulose epitopes were found in the PM. Pectin epitopes in mature vessels were highly concentrated in the annulus, a restricted area of the PM, whereas they were initially found in the whole PM in immature vessels. The pit border also showed a specific labelling pattern, with higher cellulose labelling compared with the secondary wall of the vessel. Ion-mediated variation of 24 % was found for hydraulic conductance.
• **Conclusions** Cellulose microfibrils, lignins and annulus-restricted pectins have different physicochemical properties (rigidity, hydrophobicity, porosity) that have different effects on the hydraulic functions of the PM, and these influence both the hydraulic efficiency and vulnerability to cavitation of the pits, including ion-mediated control of hydraulic conductance. Impregnation of the cellulose microfibrils of the PM with lignins, which have low wettability, may result in lower cavitation pressure for a given pore size and thus help to explain the vulnerability of this species to cavitation.

Key words: cavitation, plant water relations, sap flow, xylem, pit membrane, hydraulic conductance, immunolabelling, cellulose, pectin, lignin, annulus, *Populus tremula* × *alba*.

INTRODUCTION

In plants, long-distance sap transport occurs under negative pressure in xylem conduits, including tracheids and vessels. Sap flows between adjoining conduits through pits that form thin wall areas. Pits present considerable resistance to water flow as they account for ≥50 % of total xylem hydraulic resistance (Wheeler *et al*., 2005; Choat *et al*., 2006), the remaining part being accounted for by the conduit lumen. Pit membrane (PM) properties not only facilitate the passage of water between conduits, but also prevent the passage of air between them. Under water stress conditions, xylem tensions increase and cavitation can occur as a consequence of air seeding through the PM (Sperry and Tyree, 1988; Cochard, 2006). Cavitation provokes an air embolism that induces loss of hydraulic conductance and then potentially leads to organ or plant death. Resistance to cavitation is an important adaptive trait for drought tolerance (Maherali *et al*., 2004; Tissier *et al*., 2004; Choat *et al*., 2012). Therefore, pits occupy a crucial role in the water transport system of plants, and knowledge about PM properties is critical for understanding the influence of pits on the balance of safety and efficiency in vascular transport (Choat *et al*., 2008).

To date, investigations have focused mainly on pit structure. Within angiosperms, there is a strong correlation between PM thickness and resistance to both water flow and cavitation (Choat *et al*., 2008; Jansen *et al*., 2009). Pits with a thicker membrane have smaller pores, allowing them to resist air seeding while increasing hydraulic resistance. Moreover, a thicker membrane would also be stronger mechanically, which allows reduced stretching of the PM and thus less pore enlargement (Choat *et al*., 2004; Sperry and Hacke, 2004). However, not only do these functional properties of the pit (water permeability, resistance to air seeding and mechanical properties) depend on the structural properties of the PM, but the chemical properties of the pits are also critical. In addition, the ion-mediated variations in xylem hydraulic conductance have been attributed to the hydrogel properties of the PM (van Ieperen *et al*., 2000; Zwieniecki *et al*., 2001; Cochard *et al*., 2010). These authors proposed that this is due to the swelling/shrinking properties of the pectins, while other authors have attributed them to hemicelluloses or lignins (van Doorn *et al*., 2011), but without clear evidence for their

© The Author 2014. Published by Oxford University Press on behalf of the Annals of Botany Company. All rights reserved.
For Permissions, please email: journals.permissions@oup.com

Downloaded from http://aob.oxfordjournals.org/ at INRA Institut National de la Recherche Agronomique on December 2, 2014

presence. Insights on the composition of the PM are thus urgently desired for progress in understanding pit function.

The PM is composed of the middle lamella plus the primary walls from adjacent cells, which have undergone modifications. The PM would initially be made of cellulose microfibrils in a matrix of hydrated hemicelluloses and pectins. However, this is speculative and the modifications occurring during PM maturation, and thus the final composition of the mature pit, are unknown. It is generally accepted that the basic component of the PM is cellulose, evidenced by observation of cellulose microfibrils or staining reactions (Czaninski, 1972; Catesson, 1983; Jansen *et al*., 2009). The presence of pectins in the PM is probably the most debated aspect of their composition. Pectins consist of various and complex galacturonic acid-rich polysaccharides. In dicot cell walls, four covalently linked domains constitute pectin: homogalacturonan (HG), rhamnogalacturonan (RG)-I and RG-II and sometimes xylogalacturonans. Although their relative amounts vary according to the cell type, HG is usually the most abundant domain, constituting ~65 % of pectins, while RG-I constitutes 20–35 %. Xylogalacturonans and RG-II are minor components, each constituting <10 % (Mohnen, 2008). The RG-I backbone is substituted with single glycosyl residues or diverse longer chains, including galactans, arabinans and arabinogalactans. Moreover, the HG can be more or less methyl-esterified. The equilibrium between esterified carboxylic groups and free negative charges of dissociated carboxyl groups influences the swelling and hydration behaviour of pectins (Ryden *et al*., 2000), which can have functional importance for pit function. For instance, pectins have been proposed to be involved in the ion-mediated control of pit hydraulic conductance (Zwieniecki *et al*., 2001). In HG blocks of non-methylated galacturonic acid, Ca^{2+} cations cross-link antiparallel chains of pectins according to an 'egg-box' model (Grant *et al*., 1973), with influences on pectin swelling properties (Tibbits *et al*., 1998). The Ca^{2+} ion was also demonstrated to be critical for vulnerability to cavitation (Herbette and Cochard, 2010). Despite this physiological evidence for a role of pectins in the PM, there are contradictory results about the presence of pectins in mature pit. Studies using staining techniques suggested that there is pectin in the PM (Gortan *et al*., 2011), while others suggested that most of the pectin is removed from the pit during its maturation, except for highly methylated pectins (Czaninski, 1972, 1979; Catesson, 1983). This discrepancy in the literature can be explained by (1) the weak specificity and sensitivity of staining techniques, (2) the diverse composition of the PM across species and (3) the complex and diverse structure of pectins. Investigations on hemicelluloses in the PM are very scarce. It is proposed that hemicelluloses would be digested along with pectins during xylem vessel maturation (O'Brien, 1970). This has been observed for torus-bearing pits in gymnosperms (Dute *et al*., 2008; Kim *et al*., 2011), but this has not been addressed in angiosperms. Investigations probing the hemicelluloses are hindered by their chemical diversity and complexity. They consist of diverse polysaccharides with β(1–4)-linked backbones and they are chemically linked to cellulose (Scheller and Ulvskov, 2010). Their structure varies greatly depending on species and cell type. Several structural types can be distinguished: xyloglucans, (glucurono)xylans, mannans and glucomannans. The first of these is the most abundant hemicellulose in primary walls, while xylans are predominant in secondary walls. Although less abundant in vascular plants, mannans and glucomannans can be found in primary walls. The putative lignin deposition in pits has also attracted little attention. A few studies based on microspectrometry techniques have suggested that there is lignin in the PM (Boyce *et al*., 2004; Schmitz *et al*., 2008), but this needs to be confirmed with reliable and suitable tools. In angiosperms, lignins are complex phenolic polymers resulting from polymerization, mainly of three phenylpropanoid units, *p*-coumaryl (hydroxyphenyl unit, H), coniferyl (guaiacyl unit, G), and sinapyl (syringyl unit, S) alcohols (Freudenberg and Neish, 1968). The structure and condensation of lignins depend on species and cell type. Dicotyledons contain almost exclusively G and S units.

The investigation of pit composition has long been hindered by the lack of suitable approaches. The main pitfalls are the restricted location of the intervessel pits and their tiny size (a few micrometres), especially the pit membrane, which has a thickness in the range 0·2–0·3 µm. Ensuring sufficient resolution therefore precludes the use of analytical tools coupled to a light microscope such as Fourier transformed infrared (FTIR) microspectroscopy. Electron microscopy offers resolution well adapted to the unravelling of the pit membrane's architecture. Coupled with immunogold labelling, it is a valuable tool for probing pit composition.

In this study we investigated the distribution of the different wall components, including cellulose, hemicelluloses, pectins and lignins, to gain insight into the chemical composition of the intervessel PM. We performed immunogold labelling using transmission electron microscopy (TEM) in poplar with a set of antibodies raised against different epitopes for each of the main polysaccharide domains and lignins. To address the process of PM maturation, immunolabelling was carried out both on immature PM in forming vessels and on mature PM in functional vessels. From a schematic representation of the distribution of wall epitopes in the PM and data on the ion-mediated regulation of hydraulic conductance, we address the hydraulic properties of the pit.

MATERIALS AND METHODS

Plant material

Analyses were carried out on immature xylem from a hybrid poplar (*Populus tremula* × *P. alba*, clone INRA 717-1B4). Plants were multiplied clonally *in vitro*, acclimated and cultivated in a greenhouse with a controlled environment as described in Awad *et al*. (2012), with watering at field capacity. Plants developed a single, straight shoot, such that no tension wood was observed in cross-section. When the plants were 3 months old and had reached a height of 1·5–2 m, a stem section was sampled ~10 cm above the soil pots. Then, a section including the bark with the xylem area near the cambium was immediately placed in fixation solution. Another set of plants grown in the same conditions was used later for measurements of hydraulic conductance.

Ionic effect on hydraulic conductance

Hydraulic conductance was determined with a XYL'EM apparatus (Bronkhorst, Montigny-les-Cormeilles, France) on five

Downloaded from http://aob.oxfordjournals.org/ at INRA Institut National de la Recherche Agronomique on December 2, 2014

stem samples. First, samples 0·3 m long were flushed at 0·15 MPa for 5 min with ultra-pure water as a reference fluid (MilliQ Ultrapure Water System, Millipore, France). Conductance was then measured at 6–9 kPa using ultra-pure water at different times. Then, samples were flushed at 0·15 MPa for 5 min with a 50 mM KCl solution and conductance was measured at 6–9 kPa using the same solution. To test whether the ionic effect was reversible, a third flush was performed with ultra-pure water at 0·15 MPa for 5 min, and conductance was measured. Hydraulic conductance was expressed relative to conductance measured at time 0 min of the time kinetics using ultra-pure water.

Sample preparation for microscopy

Half or quarter sections including the inner bark and the xylem area near the cambium were made with a clean razor blade. Fragments were cut to a size of ~1 mm^3, such that the investigated PMs were in a wood area that was just below the cambium and had an area of no more than 1 mm^2. Fragments were then fixed in a mixture of 3 % paraformaldehyde and 0·5 % glutaraldehyde in a 0·1 M phosphate buffer (pH 7·2) for one night at 4 °C. After washing, samples were dehydrated in a graded aqueous ethanol series, progressively infiltrated with London Resin White (LRW) acrylic resin and then embedded in gelatin capsules. The resin was polymerized for 2 days at 50 °C without accelerator.

Semi-thin (1 µm) and ultra-thin sections (80–100 nm) were cut on an ultramicrotome (UC7; Leica Microsystems, Germany) equipped with a diamond knife. Ultra-thin sections were collected on nickel grids for immunolabelling or using plastic ring flotation for periodic acid–thiosemicarbazide-silver proteinate (PATAg) staining.

Light microscopy

Semi-thin sections were stained with 0·1 % thionin and 0·1 % methylene blue (Jansen *et al*., 2004). Observations were carried out using an Axiovert 135M microscope (Zeiss) equipped with a Retiga colour camera.

TEM procedures

PATAg staining. The PATAg treatment followed the method described by Thiery (1967). Ultra-thin sections were treated with 1 % aqueous periodic acid (Merck, Denmark) for 30 min. Then, they were rinsed five times in deionized water before incubation in thiosemicarbazide (0·2 %) (Merck, Denmark) diluted in 20 % acetic acid for 17 h. Sections were rinsed five times in decreasing acetic acid concentrations (20, 10, 5 and 2·5 %), four times in deionized water and stained with 1 % aqueous silver proteinate (Prolabo, France) in the dark for 30 min. After rinsing five times in deionized water, sections were mounted on copper grids before TEM observation.

Immunolabelling. The conditions of use and characteristics of primary antibodies are summarized in Table 1. For each immunolabelling, two blocks per sample were analysed. Ultra-thin sections were floated on a drop of phosphate-buffered saline (PBS) or Tris-buffered saline (Table 1) supplemented with 3 % bovine serum albumin to block non-specific labelling for 30 min. Sections were then incubated in buffer containing the primary antibodies (for dilutions see Table 1) supplemented with 1 % bovine serum albumin and 0·05 %Tween 20 for 1 h (antibodies 2F4, LM20, RU1, LM5, LM6, LM15, anti-AX1 and LM21) or 3 h (anti-S, anti-GS and anti-G) at room temperature. The sections were washed extensively in the buffer used for diluting the primary antibodies and then incubated for 1 h at

TABLE 1. *Specificities and conditions of use of antibodies and carbohydrate-binding molecules*

	Target	Animal	Origin	Buffer	Dilution	Reference
Antibodies						
{EM#}2F4	Homogalacturonan (HG)	Mouse	Prof. P. Van Cutsem	0·1 M TBS Tris/Ca/Na, pH 8·2	1/5	Liners *et al*. (1989)
{EM#}LM20	Esterified Homogalacturonan	Rat	PlantProbes	0·1 M PBS, pH 7·2	1/10	Verhertbruggen *et al*. (2009)
{EM#}RU1	Rhamnogalacturonan I backbone (RG-I)	Mouse	INRA	0·1 M PBS, pH 7·2	1/3	Ralet *et al*. (2010)
{EM#}LM5	Galactan	Rat	PlantProbes	0·1 M PBS, pH 7·2	1/10	Jones *et al*. (1997)
{EM#}LM6	Arabinan	Rat	PlantProbes	0·1 M PBS, pH 7·2	1/10	Willats *et al*. (1998)
{EM#}LM15	Xyloglucan	Rat	PlantProbes	0·1 M PBS, pH 7·2	1/5	Marcus *et al*. (2008)
{EM#}AX1	Arabinoxylan	Mouse	INRA	0·1 M PBS, pH 7·2	1/20	Guillon *et al*. (2004)
{EM#}LM21	Mannan	Rat	PlantProbes	0·1 M PBS, pH 7·2	1/5	Marcus *et al*. (2010)
{EM#}S	Non-condensed lignin homosyringyl structure	Rabbit	Dr K. Ruel	0·01 M TBS, pH 7·6; 500 mM NaCl	1/100	Joseleau *et al*. (2004)
{EM#}GS	Non condensed lignin mixed guaiacyl-syringyl structure (75 % syringyl units)	Rabbit	Dr K. Ruel	0·01 M TBS, pH 7·6; 500 mM NaCl	1/100	Joseleau and Ruel (1997, 2007)
{EM#}G	Condensed lignin homoguaiacyl substructure	Rabbit	Dr K. Ruel	0·01 M TBS, pH 7·6; 500 mM NaCl	1/100	Joseleau and Ruel (1997); Ruel *et al*. (2002)
Carbohydrate-binding modules						
{EM#}CBM28 (His-tagged recombinant protein)	Amorphous cellulose		Prof. J. P. Knox	0·1 M PBS, pH 7·2	10 µg/ml	Blake *et al*. (2006)
{EM#}CBM3a (His-tagged recombinant protein)	Crystalline cellulose		PlantProbes	0·1 M PBS, pH 7·2	10 µg/ml	Blake *et al*. (2006)
{EM#}Anti-His	His-tagged proteins	Mouse	Sigma-Aldrich	0·1 M PBS, pH 7·2	1/100	

TBS, Tris-buffered saline (TBS).

Downloaded from http://aob.oxfordjournals.org/ at INRA Institut National de la Recherche Agronomique on December 2, 2014

room temperature in darkness with secondary antibody (goat-anti-rat IgG, goat-anti-mouse IgG or goat anti-rabbit) conjugated with 1 nm colloidal gold complexes diluted 1 : 20 (v/v) in the respective buffer chosen for the primary antibodies (Table 1). Labelling with 1 nm gold conjugates was then intensified with a silver enhancement kit according to the manufacturer's instructions (Aurion, The Netherlands). After washing, the grids were stained with 2 % uranyl acetate.

In some cases, alkaline treatment was applied to sections prior to immunolabelling, Sections were incubated for 25 min at 4 °C with 50 µl of 0·05 M NaOH (pH 12·6) to de-esterify pectins and hemicelluloses.

Treatments and staining were done in duplicate for each sample. As a control, the first antibody was replaced with PBS and the secondary antibody used was goat-anti-rat IgG conjugated with 1 nm colloidal gold (Fig. 1).

Carbohydrate-binding modules. The conditions of use and characteristics of cellulose-binding modules (CBMs) are summarized in Table 1. Cellulose-specific labelling was carried out by using the His-tagged CBM3a and CBM28 followed by immunogold visualization. After incubation in blocking buffer, sections were treated with CBMs at 10 µg/ml in PBS and then with anti-histidine antibody diluted 1/100. Thereafter, sections were incubated with goat anti-mouse secondary antibody as described above.

The ultra-thin sections were examined with a JEOL JEM 1230 transmission electron microscope with an accelerating voltage of 80 kV. The density of labelling was determined with ImageJ software. Electron micrographs were taken at ×20 000

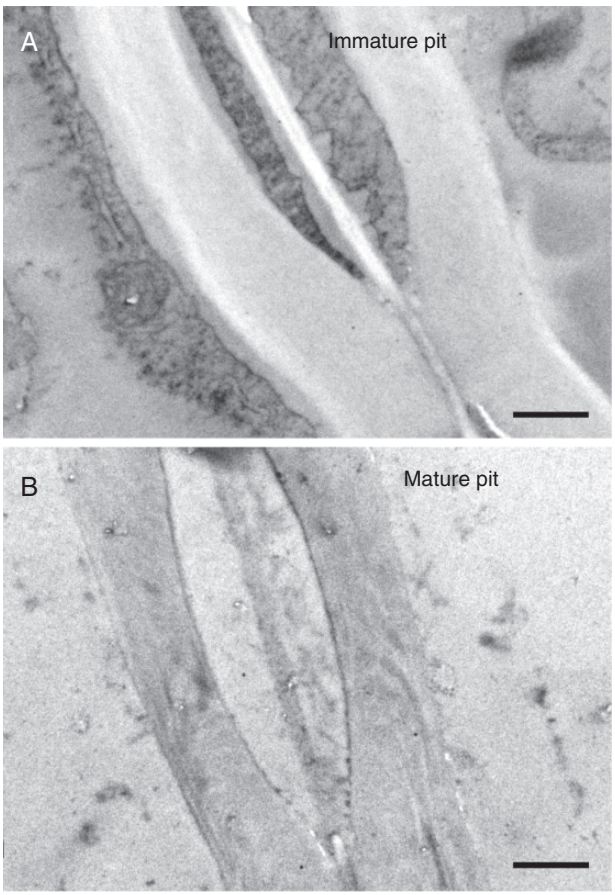

FIG. 1. Immunolabelling control. The primary antibody was replaced with PBS and the secondary antibody was goat-anti-rat IgG conjugated with 1 nm colloidal gold. (A) Immature pit. (B) Mature pit. No labelling was observed. Scale bar = 1 µm.

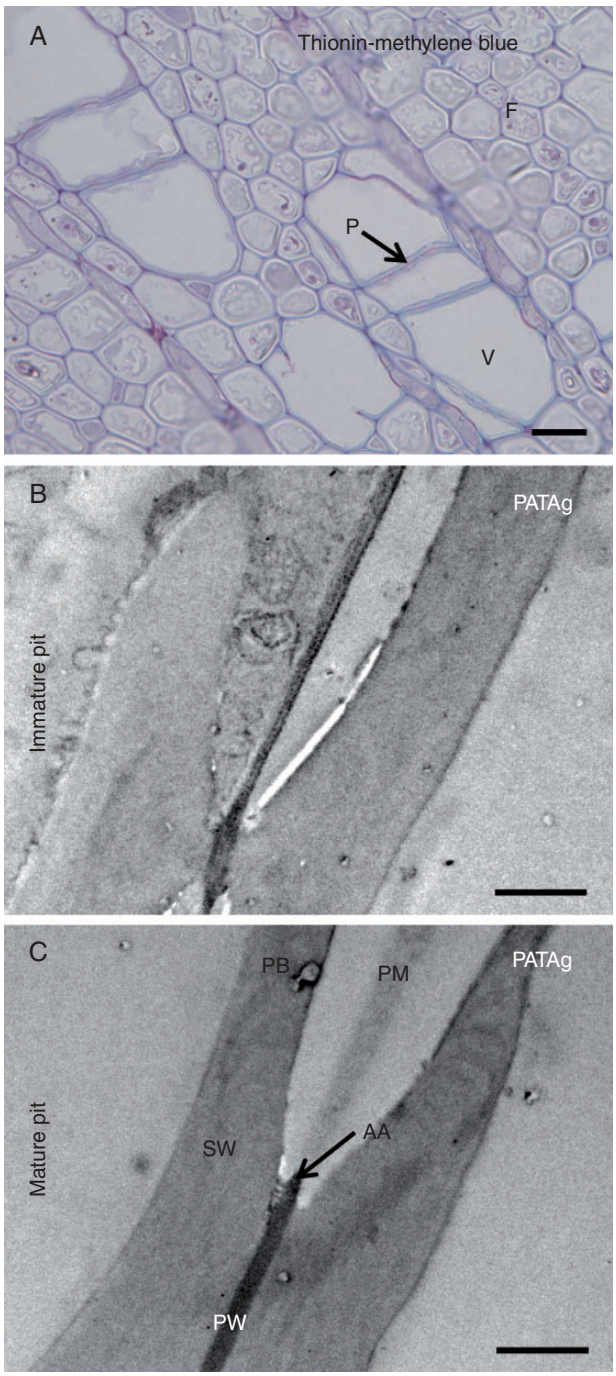

FIG. 2. Morphology of intervessel pits. (A) Thionin–methylene blue staining in light microscopy. F, fibres, P, pit, V, vessels. Scale bar = 20 µm. (B, C) PATAg staining in TEM. (B) Immature pit. (C) Mature pit. The membrane is highly labelled in the immature pit; the primary wall is strongly stained in both immature and mature pits. AA, annulus; PB, pit border; PM, pit membrane; PW, primary cell wall plus middle lamella; SW, secondary wall. Scale bars (B, C) = 1 µm.

Downloaded from http://aob.oxfordjournals.org/ at INRA Institut National de la Recherche Agronomique on December 2, 2014

magnification. For each labelling and for each state of maturation, eight to ten intervessel pits were chosen. Then, for each selected pit, the PM area and number of gold particles were measured and the density of gold particles (number/μm^2) was calculated.

RESULTS

Ultrastructure and PM immunolabelling

We focused our analyses on intervessel pits (Fig. 2A). Immature pits with remaining cell contents (Fig. 2B) were compared with mature pits connecting empty cells (Fig. 2C). The former were selected just below the cambium, while the latter were found inside the xylem. The ultrastructure of pit membranes was checked by the use of PATAg staining. Immature PM appeared thin and was strongly stained (Fig. 2B) while mature PM was less reactive to PATAg (Fig. 2C). In both immature and mature pits, the annulus strongly reacted with PATAg. These results support changes in the chemical composition of the PM during maturation.

To further investigate the composition of immature and mature PMs, labelling with affinity probes using either CBM or antibodies was carried out.

Cellulose was probed using the carbohydrate-binding modules CBM28 and CBM3a, directed against amorphous and crystalline cellulose, respectively (Table 1, Fig. 3). Weak labelling was observed in immature PMs with either probe (Fig. 3A and 3C). The PM of mature pits contained both amorphous (17 ± 5 gold particles/μm^2, Fig. 3B) and crystalline cellulose (28 ± 7 gold particles/μm^2, Fig. 3D), as did the secondary wall of vessels. The layered composition of the PM can be observed in Fig. 3D.

Immunolocalization of pectic structures was visualized using antibodies directed against different pectin motifs (Table 1). The presence of HG epitopes in cell walls, whatever their original methyl-esterification status, was studied using 2F4 antibody after alkaline de-esterification of sections. In immature pits, 2F4 antibody labelled the middle lamella primary wall very strongly in the PM (116 ± 34 gold particles/μm^2), particularly at the edge (the annulus part) (Fig. 4A). In mature pits, HG labelling was only seen in the annulus area (Fig. 4B). No labelling was found in pit borders whatever the pit status. The degree of methyl-esterification of HG was further investigated using 2F4 without alkaline pre-treatment of sections and LM20. Antibody 2F4 provides information on the spatial distribution of non-methyl-esterified galacturonic acid blocks dimerized by calcium while LM20 is indicative of highly methyl-esterified HG. The immature PM was labelled with the two antibodies (Fig. 4C and E). Blocks of unmethyl-esterified HG in the presence of calcium were evidenced with 2F4 labelling (Fig. 4C, 25 ± 8 gold particles/μm^2). They co-existed with highly methyl-esterified HG, as indicated by strong labelling with LM20 (Fig. 4E, 82 ± 22 gold particles/μm^2). In mature PM, no 2F4 labelling was observed (Fig. 4D) and LM20 labelling was only seen in the annulus area of the pit (Fig. 4F).

The RG-I domains were located using the INRA RU1 antibody, which recognizes epitopes of the RG-I backbone, and LM5 and LM6 antibodies, which recognize epitopes of the galactan and arabinan side chains, respectively (Table 1, Fig. 5). The RU1 epitope was detected in the immature PM (68 ± 11 gold particles/μm^2, Fig. 5A). In mature pits, labelling was confined to the annulus area (Fig. 5B). With anti-galactan LM5

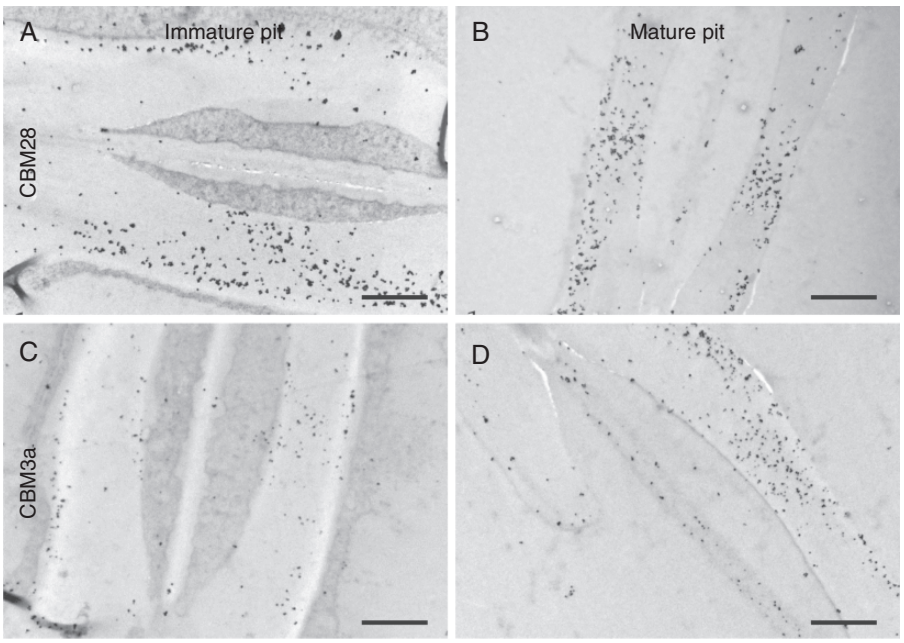

FIG. 3. Immunogold labelling of amorphous and crystalline cellulose in pits of poplar. (A, B) CBM28 labelling. (C, D) CBM3a labelling. The immature PM (A, C) showed weak labelling with either CBM28 or CBM3a, whereas labelling was stronger in the mature PM (B, D). Labelling was heterogeneous in the pit wall with both probes. In the immature pit, labelling was less dense with CBM3a. Scale bars = 1 μm.

Downloaded from http://aob.oxfordjournals.org/ at INRA Institut National de la Recherche Agronomique on December 2, 2014

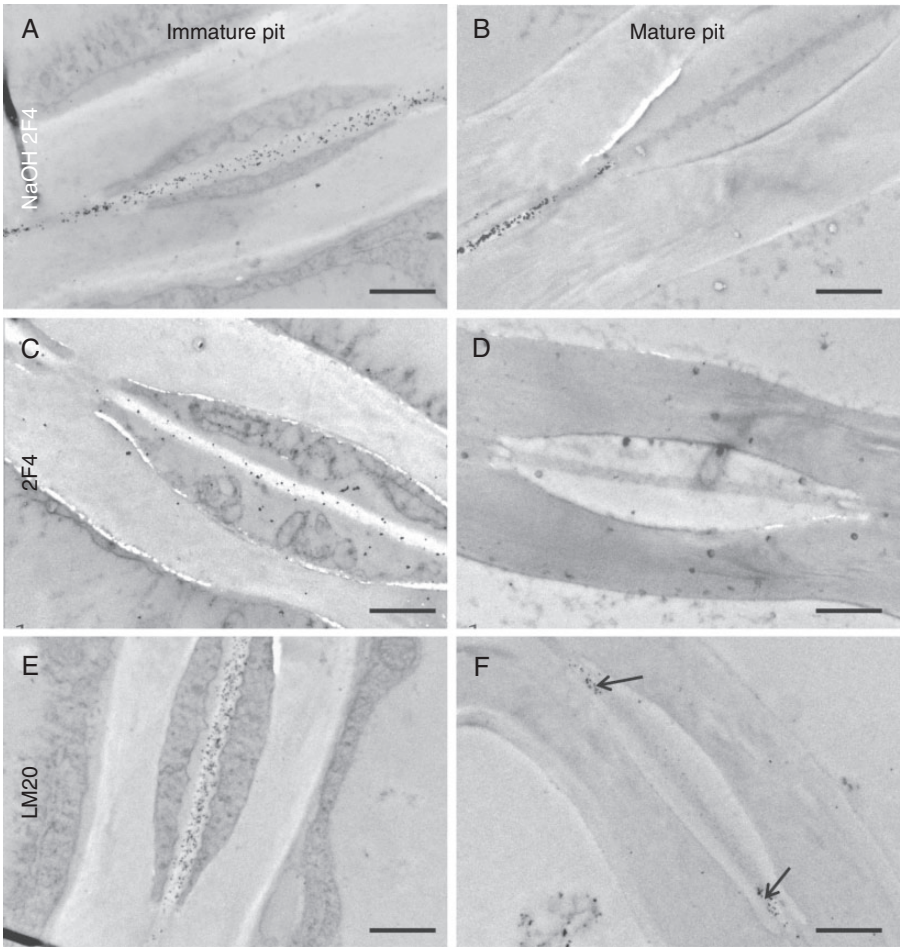

FIG. 4. Immunogold labelling of homogalacturonan epitopes in pits of poplar. (A, B) Labelling with antibody 2F4 after alkaline pre-treatment of sections. (C, D) Labelling with 2F4 without alkaline treatment. (E, F) Labelling with antibody LM20. In all cases, labelling was observed in the immature PM (A, C, E) but absent in mature pits (B, D, F). Labelling with LM20 was very strong in immature pits but was present only in the annulus area of mature pits (F, arrows). Scale bars = 1 μm.

antibody almost no labelling was detected whatever the pit status (Fig. 5C and 5D). With the anti-arabinan antibody LM6, only weak labelling was found in the primary wall outside the pit (Fig. 5F).

In conclusion, the use of a panel of antibodies targeted to different pectin domains showed that HG with various degrees of methyl-esterification and an RG-I backbone coexist in the immature PM, while side chains appear to be absent. In the mature pit, pectin epitopes are restricted to the annulus area.

The distribution of xyloglucans, arabinoxylans and mannans epitopes was analysed using the LM15, anti-AX1 and LM21 monoclonal antibodies, respectively (Table 1, Fig. 6). No labelling was seen on the immature and mature PM regardless of antibody specificity. In contrast, the AX1 epitope was abundant in the borders of both immature and mature pits (Fig. 6C, D) and the presence of mannan epitopes was detected in the borders of mature pits (Fig. 6F).

The presence of lignins in pits was studied using antibodies directed against various structural features of lignins (Table 1, Fig. 7). Epitopes of condensed lignin were visualized using anti-G antibody and epitopes of non-condensed lignin were detected with anti-GS, which primarily recognizes β-O-4 linked units, and with anti-S, which binds to the epitope of the homosyringyl substructure. The secondary walls of the pit borders were strongly labelled with the three antibodies directed against lignin substructures. The immature PM was not labelled whatever the antibody (Fig. 7A, C, E). The mature PM reacted with the three antibodies [anti-S, 70 ± 10 gold particles/μm^2 (Fig. 7B); anti-GS, 26 ± 5 gold particles/μm^2 (Fig. 7D); anti-G, 8 ± 2 gold particles/μm^2 (Fig. 7F)]. The PM would thus undergo lignification during maturation, and non-condensed lignins and, to a lesser extent, condensed lignins coexist in mature PM.

Ionic effect on xylem conductance

The effect of sap ionic strength on hydraulic conductance has been attributed to the presence of pectins in the PM (Zwieniecki *et al.*, 2001). The lack of pectin labelling demonstrated here in the mature PM of poplar vessels raises the question of this ionic effect in this species. Moreover, an ionic

Downloaded from http://aob.oxfordjournals.org/ at INRA Institut National de la Recherche Agronomique on December 2, 2014

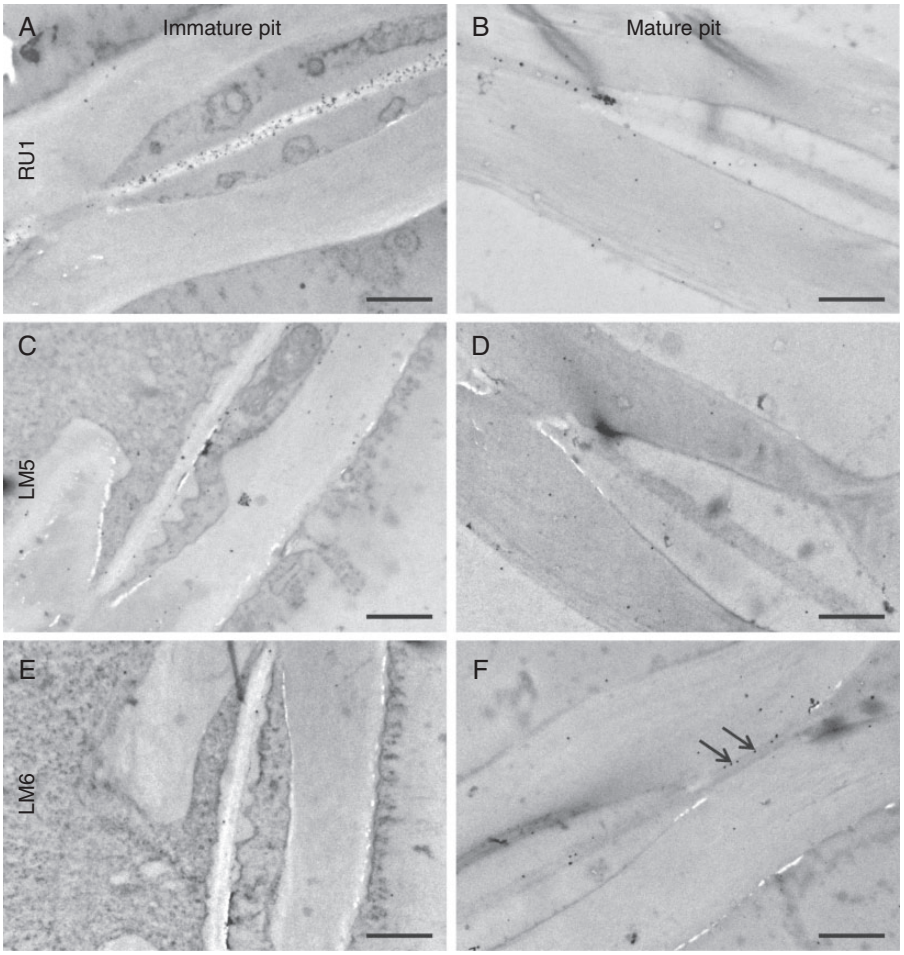

FIG. 5. Immunogold labelling of rhamnogalacturonan, galactan and arabinan epitopes in pits of poplar. (A, B) Labelling with antibody RU1 after alkaline pre-treatment of sections. (C, D) Labelling with antibody LM5. (E, F) Labelling with antibody LM6. In the immature PM, only labelling with RU1 was present (A). There was no labelling in the mature PM with RU1, LM5 and LM6 (B, D, F), except for RU1 in the annulus area (B). Labelling with LM6 (F, arrows) was found in the primary wall out of the pit. Scale bars = 1 μm.

effect on conductance did not occur in all tree species, and where it occurred it did so to various extent. Because such an effect had not been reported so far in poplar, we decided to analyse it here. Figure 8 shows the time-course of xylem conductance while perfusing with pure water or 50 mM KCl solution. Branch segments 30 cm long were first perfused with pure water under high pressure (150 kPa) and xylem conductance was then measured under low pressure (6 kPa). Xylem conductance was found to be stable. Then, the samples were perfused with 50 mM KCl solution under high pressure and conductance was measured again under low pressure. An increase of 24 % was found. After a third perfusion with pure water, xylem conductance was decreased to reach a level that was 11 % lower than the initial value. Thus, there was a strong ionic effect on hydraulic conductance in poplar, compared with many other investigated species, despite the lack of pectin epitopes in the mature PM.

DISCUSSION

Our study revealed changes in composition of the intervessel PM during maturation. Moreover, the composition demonstrated by immunolabelling, together with hydraulic properties, raises questions about the role of the membrane in conductance.

PM composition and maturation

The different stages of pit maturation have never been clearly identified. Instead of analysing several pits at different maturation stages, this study was focused on a great number of samples with counts in order to compare more accurately two contrasted stages, referred to as mature and immature pits. To analyse PM maturation, we thus compared PMs separating functional vessels having no cell content with PMs separating immature vessels still having a cell content. The PATAg staining of the immature PM was similar to that of the adjacent primary wall (Fig. 2B), whereas it was weaker in the mature PM (Fig. 2C). This is consistent with the hydrolysis of polysaccharides in the PM at the time of cell death (O'Brien, 1970), and allows investigation of the process of PM maturation. The assumed distribution of wall polysaccharides and lignins in immature and mature pits is schematized in Fig. 9. According to

Downloaded from http://aob.oxfordjournals.org/ at INRA Institut National de la Recherche Agronomique on December 2, 2014

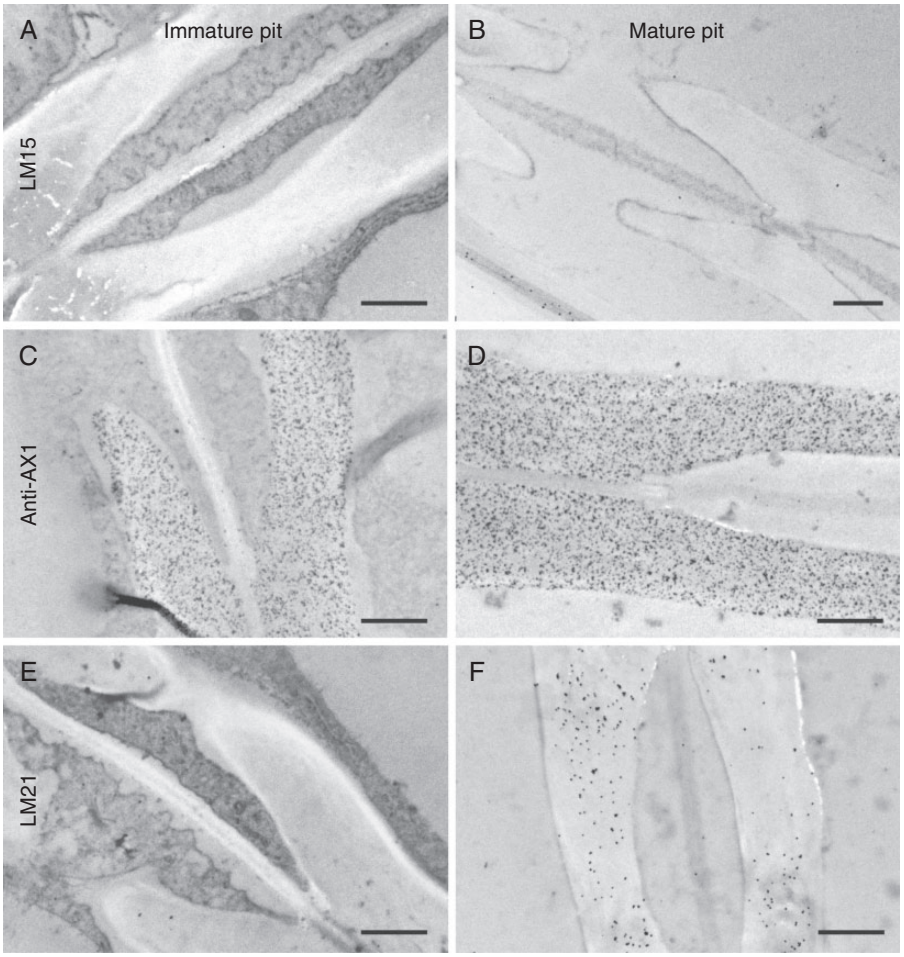

FIG. 6. Immunogold labelling of hemicellulose epitopes after alkaline pre-treatment of sections of pits of poplar. (A, B) Labelling with antibody LM15. (C, D) Labelling with anti-AX1 antibody. (E, F) Labelling with antibody LM21. No labelling of immature and mature PM was seen with antibodies against hemicelluloses. There was labelling with LM15 in the primary wall of the vessel but outside the pit (B). The secondary wall of immature and mature pits was strongly labelled with anti-AX1 (C, D), whereas LM21 epitope was detected in the secondary wall of the mature pit (F). Scale bars = 1 μm.

the labelling results, three wall regions can be distinguished in the mature pit: (1) the secondary wall of the pit border; (2) the central part of the PM, which lacks HG and rhamnogalacturonan epitopes, and (3) the annulus area of the PM, which contains blocky, unesterified HG associated with calcium, highly esterified HG and rhamnogalacturonan. In the PM, crystalline cellulose was mainly detected using CBM3a in the primary wall and not in the middle lamella.

The composition of the PM differs from that of other parts of the vessel primary wall. Before maturation, the PM was composed essentially of pectin epitopes and cellulose structures, but no hemicellulose epitopes with xyloglucans and xylans were found. Kim *et al*. (2012) reported the presence of highly substituted *O*-acetyl-4-0 methylglucuronoxylans in differentiating secondary xylem cells of aspen based on an immunolabelling experiment with LM11. They were not detected in the mature PM. The specificity of the anti-AX1 antibody we used in our experiment is closely similar to that of LM11 (Koutaniemi *et al*., 2012), but in our study we failed to detect significant labelling of the membrane in immature pits. Xyloglucans and xylans are probably hydrolysed early and thus cannot be observed on the immature vessels we studied here. Supporting this assumption, mannans were degraded in the tracheid PM during the early steps of pit formation, at the time when secondary wall deposition was still incomplete (Kim *et al*., 2011). The immature PM was composed of highly methylated HG and RG-I containing few arabinan side chains (Figs 3 and 4). During maturation, all pectin domains were likely removed to be replaced by lignins and cellulose, except in the annulus PM. Despite the absence of labelling for different pectin epitopes (2F4, LM20, RU1), we cannot rule out masking by lignins or the removal of calcium and methyl esters from pectins. The annulus PM showed the strongest pectin labelling and PATAg staining, indicating a high polysaccharide concentration. This separate and conspicuous region of the PM has previously been observed by TEM in several species (Schmid and Machado, 1968; Jansen *et al*., 2009). Using another set of antibodies (JIM5 and JIM7), Plavcova and Hacke (2011) also found that HG epitopes were not present in the main part of the PM, but were concentrated in the annulus part in the four species they investigated. Both crystalline and amorphous cellulose and lignins were found in the PM as well as in all of the vessel wall. The strong response to CBM3a supports the highly crystalline organization of cellulose in the PM. This result is in agreement

Downloaded from http://aob.oxfordjournals.org/ at INRA Institut National de la Recherche Agronomique on December 2, 2014

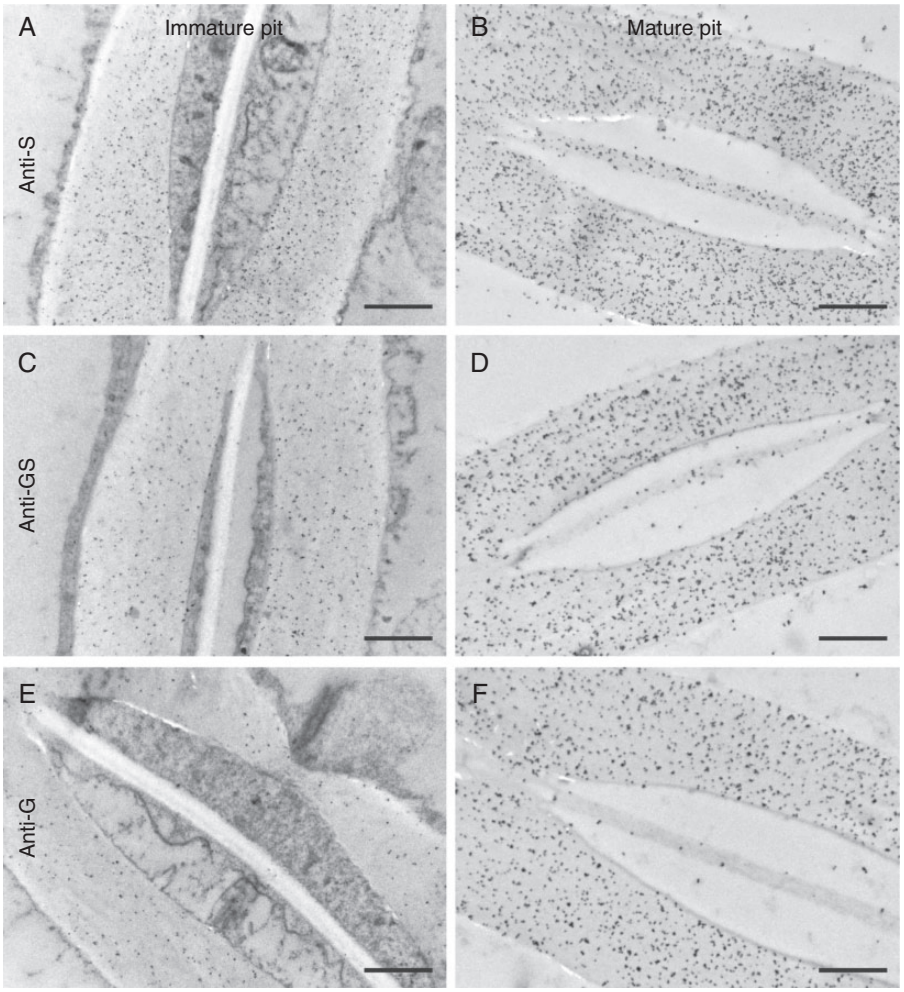

FIG. 7. Immunogold labelling of lignin epitopes in pits of poplar. (A, B) Anti-S antibody. (C, D) Anti-GS antibody. (E, F) Anti-G antibody. The secondary wall of the pit was strongly labelled with the three antibodies. The immature PM (A, C, E) was not labelled with any antibody, while the mature PM showed much higher labelling with antibodies directed against non-condensed forms of lignin structures (anti-S and anti-GS). Scale bars = 1 μm.

with observations reported on arabidopsis metaxylem by Ruel *et al*. (2012). The mutual influence of lignins and cellulose microfibrils in the development of normal secondary cell wall structure had already been emphasized in arabidopsis (Ruel *et al*., 2009) and poplar (Ruel *et al*., 2006). Lignin structures would participate in cellulose microfibril assembly and cohesion. The mature intervessel PM was rather rich in non-condensed lignins, whereas the compound middle lamella between cells was found to be rich in condensed lignin and the secondary wall was rich in non-condensed lignin, using the same antibodies (Joseleau and Ruel, 2007). Once again, the composition of the intervessel PM appeared different from that of the compound middle lamella of cells, suggesting that the two types of lignins play different roles in their respective walls.

Immunolabelling has the advantage of providing direct evidence for the presence of a compound but its usefulness can be hindered by limited accessibility of the epitope. To overcome this pitfall, we used a set of probes raised against different epitopes for each wall polysaccharide and lignins: five for pectins, three for hemicelluloses, three for cellulose and three for lignins. Moreover, additional immunofluorescence labelling was carried out on cross-sections, pre-treated or not, with a pectin lyase (Supplementary Data Fig. S1). Labelling of cellulose structures with CBM3a was shown on pre-treated as well as non-pre-treated sections, confirming the presence of crystalline cellulose. On the other hand, no labelling was observed when AX1 antibody was used on pre-treated and non-pre-teated PMs (Supplementary Data Fig. S1). Antibodies LM15 and LM21 did not show any labelling in any part of the pre-treated and non-pre-teated xylem (data not shown). This supports the absence of hemicellulose epitopes (xylans, xyloglucans and mannans) in the PM. Taken as a whole, the immunolabelling results made it possible to distinguish two chemical regions in the mature PM: the annulus PM consists of lignins and has a high concentration of pectins, while the larger and central PM part is exclusively composed of two cellulose sheets embedded in lignins.

Hydraulic properties of the PM

Because sap flows through the PM, it is rather surprising that the cellulose microfibrils of the PM were impregnated with

Downloaded from http://aob.oxfordjournals.org/ at INRA Institut National de la Recherche Agronomique on December 2, 2014

lignins and that the inner part was composed mainly or exclusively of lignins. Lignins have low wettability (Laschimke, 1989) and thus they waterproof the vessel wall such that the sap flows only across pits (Siau, 1984; McCann, 1997). Crystalline cellulose, which was prominent in the PM, was also found to have lower wettability than amorphous cellulose (Sumi *et al.*, 1964). The hydrophilic interactions between the water sap and the wall of the PM pores would thus be reduced, leading to weakening of the hydraulic resistance of the PM pore. Similarly, low wettability of the vessel wall was proposed to explain the efficient sap transport through lumen vessels (Zimmermann *et al.*, 2004). This hydraulic property of the PM needs the membrane to have a porous structure. This porous structure is supported by previous analyses based on air seeding and scanning electron microscopic observations of different trees species, including poplar (Jansen *et al.*, 2004).

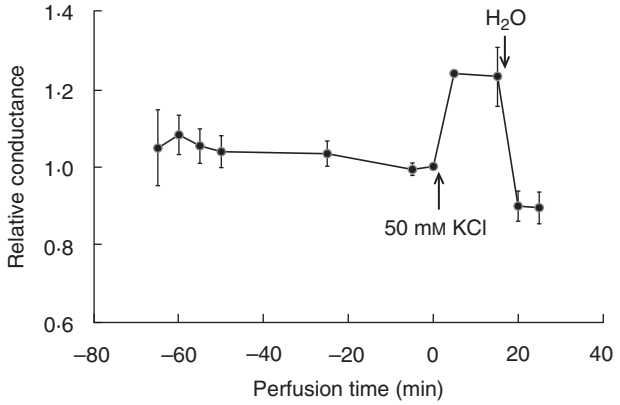

FIG. 8. Time course of relative hydraulic conductance when the stem was perfused with pure water or 50 mM KCl. Stem segments 0·3 m long were perfused with pure water and conductance was measured at different times. After time 0 min, segments were flushed then perfused with 50 mM KCl (arrow) and conductance was measured. After 15 min of perfusion, stems were flushed then perfused with pure water and conductance was again measured. Data are mean values from five samples and bars represent standard errors.

We observed an increase in xylem hydraulic conductance with increasing sap ionic concentration, in agreement with previous studies in other species (van Ieperen *et al.*, 2000; Zwieniecki *et al.*, 2001; Cochard *et al.*, 2010). This ionic effect has been attributed to the hydrogel properties of PM pectins (Zwieniecki *et al.*, 2001) and to any other polyelectrolytes of the PM (van Doorn *et al.*, 2011), but without clear evidence for their presence. Here, we demonstrated that the PM is mainly composed of cellulose coated with lignins. Thus, the hypothesis of a hydrogel effect on conductance can be ruled out. According to van Doorn *et al.* (2011), any polyelectrolyte in the wall pit pore would generate an electro-viscous effect that would make a layer of water that is less mobile and more viscous, resulting in a decrease in conductance. The range of this effect would depend on the PM pore diameter, the ionic strength of the fluid and the electric potential of the wall surface. This last parameter is related to its density of chargeable sites and thus to its polyelectrolyte composition. Recently, a theoretical investigation was conducted on the impact of electro-viscosity on the hydraulic conductance of PM pores (Santiago *et al.*, 2013). According to this study, cellulose fibres in the wall PM would harbour too low a density of chargeable sites, which would result in a very weak ionic effect on hydraulic conductance. The ionic effect on hydraulic conductance we observed was in the range of that predicted for kraft lignin or pectin extracts (Santiago *et al.*, 2013). Since no hemicelluloses

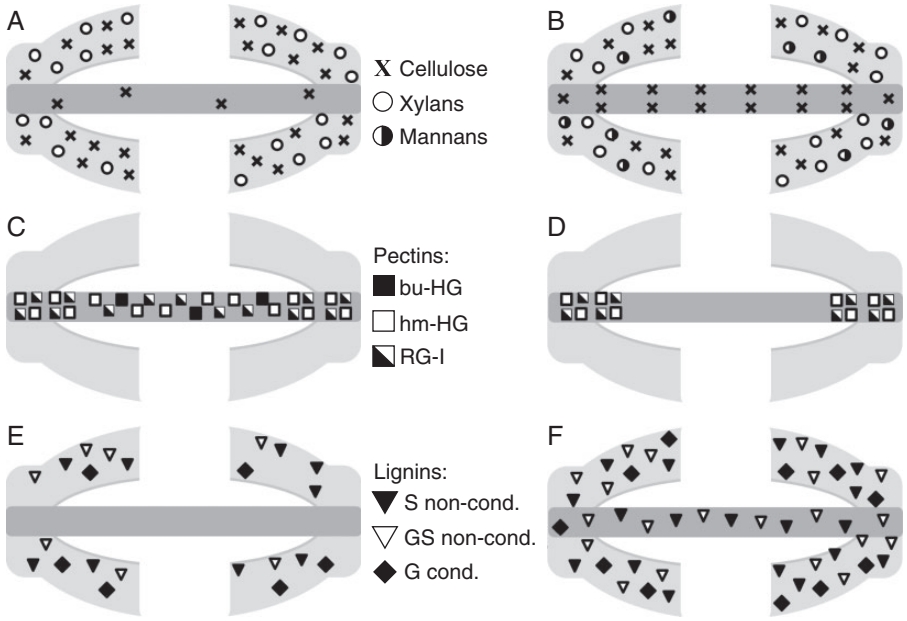

FIG. 9. Schematic representation showing the occurrence of epitopes of wall polysaccharides and lignins in pits of poplar. The distribution of epitopes seen in immunolabelling experiments is shown for immature pits between differentiating vessels (A, C, E) or mature pits between functional vessels (B, D, F). The dark grey bar represents the middle lamella plus the primary walls of adjoining cells. (A, B) Distribution of crystalline cellulose (CBM3a), xylans (AX1) and mannans (LM21). (C, D) Distribution of the pectin domains blocky-unmethylated (bu-)HG (2F4), highly methylated (hm-)HG (LM20) and RG-I (RU1). (E, F) Distribution of non-condensed lignin structures (anti-S and anti-GS). An antibody raised against condensed G lignin structures (anti-G) was also used.

Downloaded from http://aob.oxfordjournals.org/ at INRA Institut National de la Recherche Agronomique on December 2, 2014

were detected in the PM and pectin epitopes were only found in the annulus part, the ionic effect on hydraulic conductance is assumed to relate to the lignins. Indeed, lignins can harbour chargeable sites on the few phenolic hydroxyl groups that remain free. Alternatively, the ionic effect could be explained by an increase in carboxyl groups of galacturonic acids resulting from the removal of calcium bridges and methyl esters from pectins during PM maturation.

The composition of the PM can influence vulnerability to cavitation in different ways (Lens *et al*., 2013). According to the Young–Laplace law ($P = -4T.\cos\theta/D$), the xylem pressure (P) threshold needed for air seeding depends on the PM pore diameter (D), the surface tension of the sap (T) and the contact angle (θ) between the PM wall and the sap. The value of θ is usually considered to be 0, assuming a large wettability of the PM pore (Sperry and Tyree, 1988; Cochard, 2006; Jansen *et al*., 2009). This seems unlikely for poplar since cellulose and lignins would result in a non-zero contact angle and thus a lower cavitation pressure for a given pore size (Meyra *et al*., 2007). Such PM biochemistry holds for this species, in which xylem is vulnerable. A different PM composition can be expected for species with higher resistance to cavitation, as suggested by TEM investigations (Jansen *et al*., 2009). Thinning of the PM is observed in vulnerable species, whereas thickening is observed in resistant species, supporting a difference in the events occurring during pit maturation.

The mechanical behaviour of the PM has also to be considered when studying the resistance of vessels to air seeding (Choat *et al*., 2004, 2008; Sperry and Hacke, 2004). Indeed, a pressure difference between an air-filled and a sap-filled vessel stretches and deforms the PM, enlarging or creating pores in it. Sperry and Hacke (2004) demonstrated how the pit structure influences the stretching of the PM, but its intrinsic properties were not properly taken into account. They postulate that the mechanical properties rely on cellulose microfibrils. Lignins covering the PM would provide additional rigidity and compressive strength (Niklas, 1992; Chabannes *et al*., 2001), and thus increase resistance to cavitation. This would explain why transgenic poplar lines with modified lignin composition were more vulnerable to cavitation (Awad *et al*., 2012). The enzymatic hydrolysis of pectins induced a sharp increase in xylem vulnerability to cavitation in poplar (Dusotoit-Coucaud *et al*., 2014) and calcium was found to be critical for resistance to cavitation (Herbette and Cochard, 2010; Plavcova and Hacke, 2011). Yet pectin was only found clustered in the PM annulus. The most likely hypothesis is that pectins have a role in the mechanical resistance of the PM.

Our conclusions are based on the assumptions that xylem hydraulic conductance and vulnerability to cavitation are limited to vessels. However, wood fibres can also play a role in hydraulic properties. For example, two reports demonstrate the presence of water in wood fibre lumina, suggesting that they are conductive (Umebayashi *et al*., 2008, 2010). If so, investigations on fibre-vessel pits could also be considered.

Further prospects

Our results hold for poplar, in which xylem hydraulics is rather efficient but vulnerable. Variability in PM composition can be expected according to species. We found evidence that the PM in poplar xylem was mostly composed of cellulose embedded in a lignin matrix, whereas the PM in a conifer xylem contains cellulose with pectin (Maschek *et al*., 2013). Thus, the next step will be to investigate PM composition by immunolabelling in species with contrasting xylem hydraulics.

Cellulose, lignins and pectins have different physicochemical properties (rigidity, hydrophobicity, porosity) that would affect the hydraulic functions of the PM differently. Experimental demonstrations are needed to validate the hypotheses we have formulated about these functions. Now that the composition of the pits has been elucidated, the next step will be to investigate their hydraulic properties in microfluidic experiments using biomimetic membranes.

SUPPLEMENTARY DATA

Supplementary data are available only at www.aob.oxfordjournals.org and consist of Fig. S1: immunofluorescence labelling of cellulose and xylans in intervessel pits of poplar xylem before and after pre-treatment of sections with pectin lyase.

ACKNOWLEDGEMENTS

We gratefully acknowledge the gift of antibodies and CBM28 from Professor Paul Knox, Professor P. Van Cutsem and Dr Katia Ruel. We also thank Dr Katia Ruel for instructions and helpful comments regarding lignin labelling. This research was funded by the PitBulles project (ANR No. 2010 Blan 171001).

LITERATURE CITED

Awad H, Herbette S, Brunel N, *et al*. 2012. No trade-off between hydraulic and mechanical properties in several transgenic poplars modified for lignins metabolism. *Environmental and Experimental Botany* **77**: 185–195.

Blake AW, McCartney L, Flint JE, *et al*. 2006. Understanding the biological rationale for the diversity of cellulose-directed carbohydrate-binding modules in prokaryotic enzymes. *Journal of Biological Chemistry* **281**: 29321–29329.

Boyce CK, Zwieniecki MA, Cody GD, *et al*. 2004. Evolution of xylem lignification and hydrogel transport regulation. *Proceedings of the National Academy of Sciences of the USA* **101**: 17555–17558.

Catesson A. 1983. A cytochemical investigation of the lateral walls of *Dianthus* vessels. Differentiation and pit-membrane formation. *IAWA Bulletin* **4**: 89–101.

Chabannes M, Ruel K, Yoshinaga A, Chabbert B, Jauneau A. 2001. *In situ* analysis of lignins in transgenic tobacco reveals a differential impact of individual transformations on the spatial patterns of lignin deposition at the cellular and subcellular levels. *Plant Journal* **28**: 271–282.

Choat B, Jansen S, Zwieniecki MA, Smets E, Holbrook NM. 2004. Changes in pit membrane porosity due to deflection and stretching: the role of vestured pits. *Journal of Experimental Botany* **55**: 1569–1575.

Choat B, Brodie TW, Cobb AR, Zwieniecki MA, Holbrook NM. 2006. Direct measurements of intervessel pit membrane hydraulic resistance in two angiosperm tree species. *American Journal of Botany* **93**: 993–1000.

Choat B, Cobb AR, Jansen S. 2008. Structure and function of bordered pits: new discoveries and impacts on whole-plant hydraulic function. *New Phytologist* **177**: 608–625.

Choat B, Jansen S, Brodribb TJ, *et al*. 2012. Global convergence in the vulnerability of forests to drought. *Nature* **491**: 752–755.

Cochard H. 2006. Cavitation in trees. *Comptes Rendus de Physique* **7**: 1018–1026.

Downloaded from http://aob.oxfordjournals.org/ at INRA Institut National de la Recherche Agronomique on December 2, 2014

Cochard H, Herbette S, Hernandez E, Holtta T, Mencuccini M. 2010. The effects of sap ionic composition on xylem vulnerability to cavitation. *Journal of Experimental Botany* **61**: 275–285.

Czaninski Y. 1972. Observations ultrastructurales sur l'hydrolyse des parois primaries des vaisseaux chez le *Robinia pseudo-acacia* L. et l'*Acer pseudoplatanus* L. *Comptes Rendus de l'Académie des Sciences (Paris)* **275**: 361–363.

Czaninski Y. 1979. Cytochimie ultrastructurel des parois du xylème secondaire. *Biology of the Cell* **35**: 97–102.

van Doorn WG, Hiemstra T, Fanourakis D. 2011. Hydrogel regulation of xylem water flow: an alternative hypothesis. *Plant Physiology* **157**: 1642–1649.

Dusotoit-Coucaud A, Brunel N, Tixier A, Cochard H, Herbette S. 2014. Hydrolase treatments help unravel the function of intervessel pits in xylem hydraulics. *Physiologia Plantarum* **150**: 388–396.

Dute R, Hagler L, Black A. 2008. Comparative development of intertracheary pit membranes in *Abies firma* and *Metasequoia glyptostroboides*. *IAWA Journal* **29**: 277–289.

Freudenberg K, Neish AL. 1968. *Constitution and biosynthesis of lignin*. New York: Springer.

Gortan E, Nardini A, Salleo S, Jansen S. 2011. Pit membrane chemistry influences the magnitude of ion-mediated enhancement of xylem hydraulic conductance in four Lauraceae species. *Tree Physiology* **31**: 48–58.

Grant GT, Morris ER, Rees DA, Smith PJC, Thom D. 1973. Biological interactions between polysaccharides and divalent cations: the egg-box model. *FEBS Letters* **32**: 195–198.

Guillon F, Tranquet O, Quillien L, Utille JP, Ortiz JJO, Saulnier L. 2004. Generation of polyclonal and monoclonal antibodies against arabinoxylans and their use for immunocytochemical location of arabinoxylans in cell walls of endosperm of wheat. *Journal of Cereal Sciences* **40**: 167–182.

Herbette S, Cochard H. 2010. Calcium is a major determinant of xylem vulnerability to cavitation. *Plant Physiology* **153**: 1932–1939.

van Ieperen W, van Meeteren U, van Gelder H. 2000. Fluid ionic composition influences hydraulic conductance of xylem conduits. *Journal of Experimental Botany* **51**: 769–776.

Jansen S, Choat B, Vinckier S, Lens F, Schols P, Smets E. 2004. Intervascular pit membranes with a torus in the wood of *Ulmus* (Ulmaceae) and related genera. *New Phytologist* **163**: 51–59.

Jansen S, Choat B, Pletsers A. 2009. Morphological variation of intervessel pit membranes and implications to xylem function in angiosperms. *American Journal of Botany* **96**: 409–419.

Jones L, Seymour GB, Knox JP. 1997. Localization of pectic galactan in tomato cell walls using a monoclonal antibody specific to (1->4)-beta-D-galactan. *Plant Physiology* **113**: 1405–1412.

Joseleau JP, Ruel K. 1997. Study of lignification by noninvasive techniques in growing maize internodes. An investigation by Fourier transform infrared cross-polarization-magic angle spinning 13C-nuclear magnetic resonance spectroscopy and immunocytochemical transmission electron microscopy. *Plant Physiology* **114**: 1123–1133.

Joseleau JP, Ruel K. 2007. Condensed and non-condensed lignins are differently and specifically distributed in the cell walls of softwoods, hardwoods and grasses. *Cellulose Chemistry and Technology* **41**: 487–494.

Joseleau JP, Faix O, Kuroda K, Ruel K. 2004. A polyclonal antibody directed against syringylpropane epitopes of native lignins. *Comptes Rendus Biologies* **327**: 809–815.

Kim JS, Awano T, Yoshinaga A, Takabe K. 2011. Temporal and spatial diversities of the immunolabelling of mannan and xylan polysaccharides in differentiating earlywood ray cells and pits of *Cryptomeria japonica*. *Planta* **233**: 109–122.

Kim JS, Sandquist D, Sundberg B, Daniel G. 2012. Spatial and temporal variability of xylan distribution in differentiating secondary xylem of hybrid aspen. *Planta* **235**: 1315–1330.

Koutaniemi S, Guillon F, Tranquet O, *et al.* 2012. Substituent-specific antibody against glucuronoxylan reveals close association of glucuronic acid and acetyl substituents and distinct labeling patterns in tree species. *Planta* **236**: 739–751.

Laschimke R. 1989. Investigation of the wetting behaviour of natural lignin – a contribution to the cohesion theory of water transport in plants. *Thermochimica Acta* **151**: 35–56.

Lens F, Tixier A, Cochard H, Sperry JS, Jansen S, Herbette S. 2013. Embolism resistance as a key mechanism to understand adaptive plant strategies. *Current Opinion in Plant Biology* **16**: 287–292.

Liners F, Letesson JJ, Didembourg C, van Custem P. 1989. Monoclonal antibodies against pectin. Recognition of a conformation induced by calcium. *Plant Physiology* **91**: 1419–1424.

Maherali H, Pockman WT, Jackson RB. 2004. Adaptive variation in the vulnerability of woody plants to xylem cavitation. *Ecology* **85**: 2184–2199.

Marcus SE, Verhertbruggen Y, Herve C, *et al.* 2008. Pectic homogalacturonan masks abundant sets of xyloglucan epitopes in plant cell walls. *BMC Plant Biology* **8**: 60.

Marcus SE, Blake AW, Benians TAS, *et al.* 2010. Restricted access of proteins to mannan polysaccharides in intact plant cell walls. *Plant Journal* **64**: 191–203.

Maschek D, Goodell B, Jellison J, Lessard M, Militz H. 2013. A new approach for the study of the chemical composition of bordered pit membranes: 4Pi and confocal laser scanning microscopy. *American Journal of Botany* **100**: 1751–1756.

McCann MC. 1997. Tracheary element formation: building up to a dead end. *Trends in Plant Sciences* **2**: 333–338.

Meyra AG, Kuz VA, Zarragoicoechea GJ. 2007. Geometrical and physicochemical considerations of the pit membrane in relation to air seeding: the pit membrane as a capillary valve. *Tree Physiology* **27**: 1401–1405.

Mohnen D. 2008. Pectin structure and biosynthesis. *Current Opinion in Plant Biology* **11**: 266–277.

Niklas K. 1992. Biomechanics and plant evolution. In: *Plant biomechanics. An engineering approach to plant form and function.* Chicago: University of Chicago Press, 474–573.

O'Brien T. 1970. Further observations on hydrolysis of the cell wall in the xylem. *Protoplasma* **69**: 1–14.

Plavcova L, Hacke UG. 2011. Heterogeneous distribution of pectin epitopes and calcium in different pit types of four angiosperm species. *New Phytologist* **192**: 885–897.

Ralet MC, Tranquet O, Poulain D, Moise A, Guillon F. 2010. Monoclonal antibodies to rhamnogalacturonan I backbone. *Planta* **231**: 1373–1383.

Ruel K, Montiel M-D, Goujon T, Jouanin L, Burlat V, Joselean JP. 2002. Interrelation between lignin deposition and polysaccharide matrices during assembly of plant cell walls. *Plant Biology* **4**: 1–7.

Ruel K, Chevalier-Billosta V, Guillemenin F, Berrio-Sierra J, Joseleau JP. 2006. The wood cell wall at the ultrastructural scale-formation and topochemical organization. *Maderas, Ciencia y Tecnologia* **8**: 107–116.

Ruel K, Berrio-Sierra J, Derikvand MM, *et al.* 2009. Impact of CCR1 silencing on the assembly of lignified secondary walls in *Arabidopsis thaliana*. *New Phytologist* **184**: 99–113.

Ruel K, Nishiyama Y, Joseleau JP. 2012. Crystalline and amorphous cellulose in the secondary walls of *Arabidopsis*. *Plant Science* **193–194**: 48–61.

Ryden P, MacDougall AJ, Tibbits CW, Ring SG. 2000. Hydration of pectic polysaccharides. *Biopolymers* **54**: 398–405.

Santiago M, Pagay V, Stroock AD. 2013. Impact of electroviscosity on the hydraulic conductance of the bordered pit membrane: a theoretical investigation. *Plant Physiology* **163**: 999–1011.

Scheller HV, Ulvskov P. 2010. Hemicelluloses. *Annual Review of Plant Biology* **61**: 263–289.

Schmid R, Machado R. 1968. Pit membranes in hardwoods – fine structure and development. *Protoplasma* **66**: 185–204.

Schmitz N, Koch G, Schmitt U, Beeckman H, Koedam N. 2008. Intervessel pit structure and histochemistry of two mangrove species as revealed by cellular UV microspectrophotometry and electron microscopy: intraspecific variation and functional significance. *Microscopy and Microanalysis* **14**: 387–397.

Siau J. 1984. *Transport processes in wood*. Berlin: Springer.

Sperry JS, Hacke UG. 2004. Analysis of circular bordered pit function I. Angiosperm vessels with homogenous pit membranes. *American Journal of Botany* **91**: 369–385.

Sperry JS, Tyree MT. 1988. Mechanism of water stress-induced xylem embolism. *Plant Physiology* **88**: 581–587.

Sumi Y, Hale R, Meyer J, Leopold A, Ranby G. 1964. Accessibility of wood and wood carbohydrates measured with tritiated water. *Tappi Journal* **47**: 621–624.

Thiery J-P 1967. Mise en évidence de polysaccharides sur coupes fines en microscopie électronique. *Journal de Microscopie* **6**: 987–1018.

Downloaded from http://aob.oxfordjournals.org/ at INRA Institut National de la Recherche Agronomique on December 2, 2014

Tibbits CW, MacDougall AJ, Ring SG. 1998. Calcium binding and swelling behaviour of a high methoxyl pectin gel. *Carbohydrate Research* **310**: 101–107.

Tissier J, Lambs L, Peltier J, Marigo G. 2004. Relationships between hydraulic traits and habitat preference for six *Acer* species occurring in the French Alps. *Annals of Forest Science* **61**: 81–86.

Umebayashi T, Utsumi Y, Koga S, Inoue S, Arakawa K, Matsumura J, Oda K. 2008. Conducting pathways in north temperate deciduous broadleaved trees. *IAWA Journal* **29**: 247–263.

Umebayashi T, Utsumi Y, Koga S, Inoue S, Matsumura J, Oda K, Fujikawa S, Arakawa K, Otsuki K. 2010. Xylem water-conducting patterns of 34 broadleaved evergreen trees in southern Japan. *Trees - Structure and Function* **24**: 571–583.

Verhertbruggen Y, Marcus SE, Haeger A, Ordaz-Ortiz JJ, Knox JP. 2009. An extended set of monoclonal antibodies to pectic homogalacturonan. *Carbohydrate Research* **344**: 1858–1862.

Wheeler J, Sperry J, Hacke U, Hoang N. 2005. Intervessel pitting and cavitation in woody Rosaceae and other vesselled plants: a basis for a safety versus efficiency trade-off in xylem transport. *Plant, Cell and Environment* **28**: 800–812.

Willats WGT, Marcus SE, Knox JP. 1998. Generation of a monoclonal antibody specific to (1-> 5)-alpha-L-arabinan. *Carbohydrate Research* **308**: 149–152.

Zimmermann U, Schneider H, Wegner LH, Haase A. 2004. Water ascent in tall trees: does evolution of land plants rely on a highly metastable state? *New Phytologist* **162**: 575–615.

Zwieniecki MA, Melcher PJ, Michele Holbrook NM. 2001. Hydrogel control of xylem hydraulic resistance in plants. *Science* **291**: 1059–1062.

Downloaded from http://aob.oxfordjournals.org/ at INRA Institut National de la Recherche Agronomique on December 2, 2014